Proceedings of the
International Conference on Mechanical Engineering and Renewable Energy 2019
(ICMERE2019) 11 – 13 December, 2019, Chittagong, Bangladesh

ICMERE2019-PI-189

NUMERICAL INVESTIGATION OF HEAT TRANSFER PERFORMANCE OF CuO/ETHYLENE GLYCOL-WATER (60:40) v/v% NANOFLUID FOR TURBULENT PIPE FLOW

Abu Raihan Ibna Ali[1], **Moham Ed Abdur Razzaq**[2*] , **Bodius Salam**[3], **and Jamal Uddin Ahamed**[4]

Department of Mechanical Engineering, Chittagong University of Engineering & Technology, Chittagong-4349, Bangladesh
abu.raihan.pilu@gmail.com[1], a.razzaq@cuet.ac.bd[2*], bsalam@cuet.ac.bd[3], jamal@cuet.ac.bd[4]

Abstract- *Ethylene glycol-water (60:40) v/v% is the common heat transfer fluid used in automotive cooling system. Heat transfer of this fluid can be enhanced by dispersing nanoparticles resulting in less pumping power for the desired heat transfer coefficient compared with base fluid. The objective of the present study is to investigate the pumping power per unit length of CuO/EG-W (60:40) v/v% nanofluid. Investigation was carried out for EG-W (60:40) v/v% and 1% volume fraction of CuO/EG-W (60:40) v/v% nanofluid flow through the pipe using ANSYS FLUENT (Academic Version). It is concluded that pumping power per unit length of CuO/EG-W (60:40) v/v% nanofluid is comparatively less than EG-W (60:40) v/v% to get the same heat transfer coefficient. And compact cooling system can be designed because of less pumping power for the same heat transfer.*

Keywords: Pumping Power, Nanofluid, Ethylene-glycol, Heat Transfer Enhancement

1. INTRODUCTION

Ethylene glycol-water mixture is the most common heat transfer fluid (HTF) used in the automotive cooling system. The volumetric ratios of ethylene glycol to the water of 60:40, 50:50 and 70:30 are generally preferred. Ethylene glycol mixed with water increases the freezing temperature of pure water. The thermophysical properties of ethylene glycol can be enhanced by dispersing nanoparticles in this base fluid which is known as nanofluid. A small quantity of nanoparticle is suspended in the base fluids such as water, ethylene glycol, etc. in which the average size of nanoparticles is below 100 nm. The thermophysical properties of the base fluid are enhanced because of the incorporation of nanoparticles which increase the heat transfer coefficient. The degree of enhancement of heat transfer depends on the volume fraction of nanoparticles. Generally, metal oxides like Al_2O_3, CuO, TiO_2, ZnO, MgO, etc. are dispersed as nanoparticles in water, ethylene glycol, etc. base fluid.

Al_2O_3/water nanofluid was investigated by Peyghambarzadeh et al. [1] in the car radiator. They found 45% heat enhancement than pure water. Nguyen et al. [2] also investigated Al_2O_3/water nanofluid of 6.8% volume concentration and found 40% increase in heat transfer coefficient. Nanofluid was studied by Choi [3] in the automotive cooling system and found satisfactory result. Xuan and Li [4] conducted an investigation of Cu nanoparticles dispersed in the water at different volume concentrations. They observed that thermal conductivity of the base fluid enhanced by 1.24 to 1.78 times. Hussein et al. [5] dispersed different metal oxides and found that Nusselt number is higher in SiO_2 nanofluid than Al_2O_3 and TiO_2 nanofluid. Hwang and Choi [6] investigated Al_2O_3 nanofluid and found that heat transfer coefficient enhances by 8% for volume concentration of 3%. Pumping power of Al_2O_3/water nanofluid in car radiator was investigated by P.A. Ingole et al. [7]. They showed that the pumping power of Al_2O_3/water nanofluid is comparatively less than pure water. Sundar et al. [8] carried out an experiment on thermal conductivity of 50:50% EG-W/CuO and 50:50% EG-W/Al_2O_3 nanofluids of different volume concentration and found that thermal conductivity increases with the increase in volume concentration of nanofluid. Besides the increase in thermal conductivity, researchers have found that Brownian motion of nanoparticles is liable in enhancement of heat transfer.

From the above literature review, it is visible that nanofluid has much importance on heat transfer enhancement. Especially, it has a potential application in the automotive cooling system. Hence, a numerical investigation has been performed with the help of ANSYS FLUENT (Academic Version) to investigate the pumping power of CuO/EG-W (60:40) v/v% nanofluid.

2. MATERIALS AND METHODS

2.1 Physical model

Circular pipe having a length of 2m and diameter of 0.028m was modeled and simulated in ANSYS. Boundary conditions were applied and solved numerically. The fluid flowing in the pipe was ethylene glycol-water and glycol-water with 1% volume concentration of CuO nanoparticles.

2.2 Mathematical modeling and data reduction

2.2.1 Thermophysical and Flow Characteristics of Nanofluid

Density of Nanofluids:

The density of a nanofluid is estimated by the classical mixture law. According to the classical mixture law, the density of nanofluid is expressed by Eq. (1),

$$\rho_{nf} = \rho_{np}\phi + (1-\phi)\rho_{bf} \tag{1}$$

Specific Heat of Nanofluids:

Specific heat of nanofluid is less than the base fluid. Experimentally, specific heat is measured by Calorimetry meter. Specific heat of nanofluid can be estimated by Eq. (2) which was proposed by Xuan and Roetzel [9]. The equation was derived assuming thermal equilibrium.

$$C_{p_{nf}} = \frac{\phi\, \rho_{np} C_{p_{np}} + (1-\phi)\, \rho_{bf} C_{p_{bf}}}{\rho_{nf}} \tag{2}$$

Where,

$$\rho_{nf} = \rho_{np}\phi + (1-\phi)\rho_{bf} \tag{3}$$

Thermal conductivity of Nanofluids:

Thermal conductivity of nanofluid can be computed from Hamilton–Crosser [10] model. The shape factor of nanoparticles was considered in this model. This model is identical with the Maxwell model when n=3.

$$\frac{k_{nf}}{k_{bf}} = \frac{k_p + (n-1)k_f - (n-1)\phi(k_f - k_p)}{k_p + (n-1)k_f + \phi(k_f - k_p)} \tag{4}$$

Where,
n= 3/ψ; ; ψ=1 for spherical

Dynamic viscosity of Nanofluids:

Dynamic viscosity of nanofluid is the function of volume concentration of nanoparticles and dynamic viscosity of the base fluid which is higher than the base fluid. Experimentally, Viscometer is used to measure the dynamic viscosity. Using Brinkman [11] model dynamic viscosity can be calculated up to volume concentration 4%.

$$\frac{\mu_{nf}}{\mu_{bf}} = \frac{1}{(1-\phi)^{2.5}} \tag{5}$$

Fluid Flow Characteristics of Nanofluids:

Dimensionless Reynolds number for the nanofluid flow is expressed as,

$$Re = \frac{\rho_{nf} V_{av} D_h}{\mu_{nf}} \tag{6}$$

For turbulent pipe flow pressure drop is calculated from Eq. (7),

$$\Delta P = \frac{f L \rho V^2}{2D_h} \tag{7}$$

The pumping power per unit length is calculated as,

$$W = \frac{\pi D^2 V_{av} \Delta P}{4L} \tag{8}$$

The friction factor is calculated from the Colebrook equation [12] by iteratively. The friction factor depends on the Reynolds number and the relative roughness ε /D. Colebrook equation is as the following equation.

$$\frac{1}{\sqrt{f}} = -2.0 \log\left(\frac{\frac{\varepsilon}{D}}{3.7} + \frac{2.51}{Re\sqrt{f}}\right) \tag{9}$$

Again, for smooth pipe in case of turbulent flow, skin factor can be calculated from Petukhov [13] correlation as,

$$f = (1.82 \log Re - 1.64)^{-2} \tag{10}$$

This equation is valid for $for\ 3000 < Re < 5 \times 10^6$

Heat transfer is calculated as,

$$Q_{nf} = m_{nf} C_{p_{nf}} (T_{bo} - T_{bi}) \tag{11}$$

Where,
T_{bi}= bulk temperature of inlet fluid
T_{bo}= bulk temperature of outlet fluid
m_{nf} = mass flow rate of nanofluid
Average heat transfer coefficient of nanofluid is as Eq. (12).

$$h_c = \frac{Q_{nf}}{A_w(\Delta T)} \tag{12}$$

Where,
$A_w = \pi D_i L$= surface area of circular tube

Log Mean Temperature Difference (LMTD) is calculated as,

$$\Delta T = \frac{(T_w - T_o) - (T_w - T_i)}{\ln\left(\frac{T_w - T_o}{T_w - T_i}\right)} \tag{13}$$

Nusselt number is defined as,

$$Nu = \frac{h_{av} D_h}{K_{nf}} \tag{14}$$

Thermal diffusivity is defined as,

$$\alpha_{nf} = \frac{K_{nf}}{\rho_{nf} C p_{nf}} \tag{15}$$

2.2.2 Governing Equation

Conservation of Mass:

Within the control volume, the total amount of mass remains constant. For steady incompressible two-dimensional flow, conservation of mass expressed as,

$$\frac{\partial u}{\partial x} + \frac{\partial v}{\partial y} = 0 \tag{16}$$

Conservation of mass equation is also known as continuity equation.

Conservation of Momentum:
For steady two-dimensional incompressible flow, conservation of momentum in the x-direction is expressed as,

$$\rho\left(u\frac{\partial u}{\partial x}+v\frac{\partial u}{\partial y}\right)=\mu\frac{\partial^2 u}{\partial y^2}-\frac{\partial P}{\partial x} \qquad (17)$$

Conservation of Energy:
The energy equation for steady two-dimensional incompressible flow can be expressed as,

$$\rho C_p\left[u\frac{\partial T}{\partial x}+v\frac{\partial T}{\partial y}\right]=k\left(\frac{\partial^2 T}{\partial x^2}+\frac{\partial^2 T}{\partial y^2}\right)+\mu\varphi \qquad (18)$$

Where φ is viscous dissipation function which is expressed as,

$$\varphi=2\left[\left(\frac{\partial u}{\partial x}\right)^2+\left(\frac{\partial v}{\partial y}\right)^2\right]+\left(\frac{\partial u}{\partial y}+\frac{\partial v}{\partial x}\right)^2 \qquad (19)$$

2.2.2 Turbulence Model

Standard k-ε model is the most widely-used engineering turbulence model which is robust and reasonably accurate. It is a semi-empirical model based on transport equations for turbulence kinetic energy and turbulent dissipation rate. Transport equation of k is derived from the exact equation, while the transport equation for ε is derived using physical reasoning. Standard k-ε model is valid only for fully developed turbulent flows. Enhanced wall function was used as ε equation contains a term which cannot be calculated without wall function.
Transport equation for turbulent kinetic energy (k) is as,

$$\frac{\partial(\rho k)}{\partial t}+\frac{\partial(\rho k u_i)}{\partial x_i}=\frac{\partial}{\partial x_j}\left[\left(\mu+\frac{\mu_t}{\sigma_k}\right)\frac{\partial k}{\partial x_j}\right]+G_k+G_b-\rho\varepsilon-Y_M+S_k \qquad (20)$$

And transport equation for turbulent dissipation rate (ε) is as,

$$\frac{\partial(\rho\varepsilon)}{\partial t}+\frac{\partial(\rho\varepsilon u_i)}{\partial x_i}=\frac{\partial}{\partial x_j}\left[\left(\mu+\frac{\mu_t}{\sigma_\varepsilon}\right)\frac{\partial\varepsilon}{\partial x_j}\right]+C_{1\varepsilon}\frac{\varepsilon}{k}(G_k+C_{3\varepsilon}G_b)-C_{2\varepsilon}\rho\frac{\varepsilon^2}{k}+S_\varepsilon \qquad (21)$$

Where, $\mu_t=\text{Turbulent viscosity}=\rho C_\mu\frac{k^2}{\varepsilon}$ (22)

G_k = Generation of the turbulent kinetic energy due to the mean velocity gradient

σ_k = Effective Prandtl number for turbulent kinetic energy

σ_ε = Effective Prandtl number for rate of dissipation

$C_{1\varepsilon}, C_{2\varepsilon}$ are constants

Model Constants:
The default values of model constants $C_{1\varepsilon}, C_{2\varepsilon}, C_\mu, \sigma_k, and\ \sigma_\varepsilon$ determined from experiments for fundamental turbulent flows and have the following values
$C_{1\varepsilon}=1.44, C_{2\varepsilon}=1.92, C_\mu=0.09, \sigma_k=1.0, \sigma_\varepsilon=1.3$

2.3 Boundary conditions

Inlet velocities of EG-W and CuO/EG-W (60:40) v/v% were given with temperature of 298K. A constant heat flux of 15000 W/m^2 was applied at the pipe wall for all simulations. The properties of EG-W (60:40) v/v% at 25 ℃ are given in table 1. All governing equations were solved in associated with the standard k-ε turbulent model. Turbulent intensity is calculated from the Eq. (23)

$$I=\frac{u'}{u_{avg}}=0.16\,Re_{D_H}^{-\frac{1}{8}} \qquad (23)$$

Table 1: Properties of EG-W (60:40)

Properties	Value
Density, ρ [kg/m^3] [14]	1083.87
Specific heat, C_p [KJ/Kg.K] [14]	3.106
Thermal conductivity, K [W/m.K] [14]	0.336
Dynamic viscosity, μ [mPa-s] [14]	4.52

Table 2: Properties of CuO

Properties	Value
Density, ρ [kg/m^3] [15]	6400
Specific heat, C_p [J/Kg.K] [15]	531
Thermal conductivity, K [W/m.K] [16]	76.5

2.4 Solution method and convergence criteria

The pipe flow was steady state and gravity independent as it was horizontal. Pressure based solver and enhanced near wall treatment were selected. Simple scheme solution method was chosen. Under spatial discretization, the gradient was Green Gauge Cell-based and second-order upwind was selected for continuity and turbulent kinetic energy. The values of other parameters under relaxation were the default. Simulations were performed till continuity, x-velocity, y-velocity, energy, k and epsilon residue reached $10^{-6}, 10^{-6}$, 10^{-9}, 10^{-9}, and 10^{-5}. Computer with 8 GB DDR4 RAM, Intel(R) Core(TM) i5-6200U CPU @ 2.30GHz (4 CPUs) processor and 2 GB NVIDIA GEFORCE graphics card were used.

2.5 Model validation
2.5.1 Grid Sensitivity Check

Simulations were performed for different grid size using the maximum grid size of 1.2*0.8 mm, 1*0.6 mm, 0.8*0.4 mm, 0.6*0.2mm, 0.4*0.1mm and 0.2*0.08 mm. Mesh were clustered near the pipe wall to detect viscous sublayer. Grid sensitivity was checked by the numerical value of friction factor for inlet velocity of 1.5 m/s for EG-W (60:40) v/v% fluid. Fig.1 illustrates that friction factor changes very little for the grid size of 0.6*0.2mm, 0.4*0.1mm and 0.2*0.08 mm. So, considering computational cost and accuracy, the maximum grid size of 0.4*0.1mm was selected for the simulations.

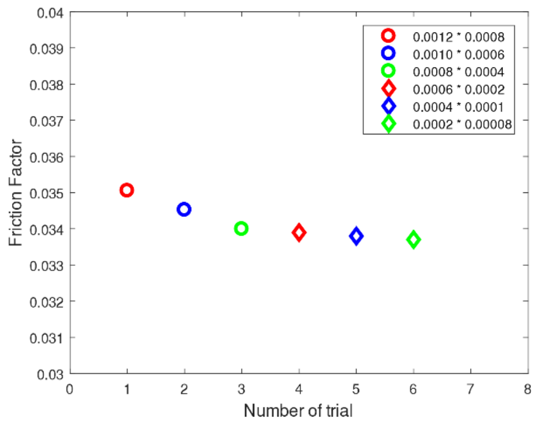

Fig. 1: Friction Factor for Different Grid Size

2.5.1 Validation of simulation

The simulation was validated by comparing the friction factor by Petukhov [13] correlation and Blasius equation. Simulated friction factor showed satisfactory agreement comparing with Petukhov correlation and Blasius equation with variation ranging from 1.2% to 7.7%. Simulation validation is illustrated in fig. 2. Nusselt number is validated by Gnielinski correlation [17] in Fig. 4.

3. PUMPING POWER OF EG-W/CuO NANOFLUIDS

Fig. 2 illustrates friction factor for different Reynold number of EG-W (60:40) v/v% and CuO/EG-W (60:40) v/v% nanofluid with a volume concentration of 1%. Friction factor decreases with the increase in Reynold number. Friction factor showed satisfactory agreement comparing with Petukhov correlation and Blasius equation with variation ranging from 1.2% to 7.7%. Fig. 2 demonstrates that friction factors of CuO/EG-W (60:40) v/v% and CuO/EG-W (60:40) v/v% nanofluid with a volume concentration of 1% are almost constant for different Reynolds number. At low volume concentration of nanofluid, there is no change in friction factor compared with base fluid.

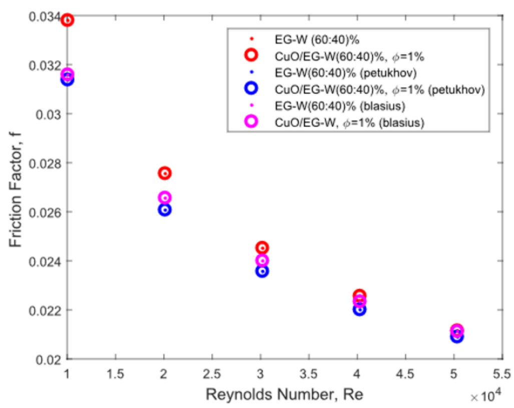

Fig. 2: Friction Factor Vs. Reynolds Number

Fig. 3 illustrates the relation of heat transfer coefficient with Reynolds number. Heat transfer coefficient increases with the increase in Reynold number both for CuO/EG-W(60:40) v/v% nanofluid and EG-W (60:40) v/v% . It is noticeable from Fig. 3 that for 1% volume fraction of nanofluid, the heat transfer coefficient is higher than EG-W (60:40) v/v%. In the case of nanofluid, the heat transfer coefficient increases because of the increase in thermal conductivity and decrease in the specific heat of nanofluid. The present work has been done only for 1% volume fraction of nanofluid. If the volume fraction of nanofluid increases, heat transfer coefficient also increases.

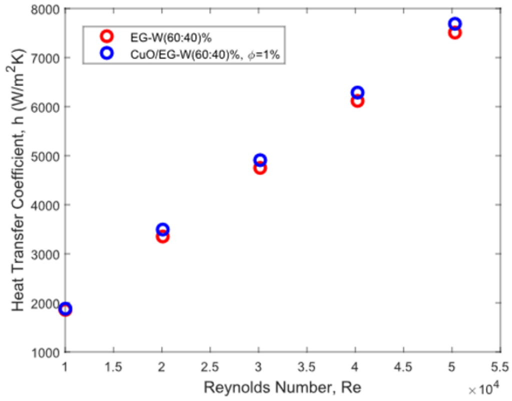

Fig. 3: Heat Transfer Coefficient Vs. Reynolds Number

Fig. 4 illustrates the relation between Nusselt number and Reynolds number of Cu/EG-W(60:40) v/v% and CuO/EG-W(60:40) v/v% nanofluid. Fig. 4 also demonstrates the Nusselt number for 1% volume fraction of CuO/EG-W(60:40) v/v% nanofluid is higher than EG-W (60:40) v/v%. The Nusselt number calculated from Dittus Boelter deviates much from Gnielinski correlation [17]. But, simulated Nusselt numbers are close to Nusselt number calculated from Gnielinski correlation for EG-W (60:40) v/v%. On the other hand, Nusselt number of 1% volume fraction CuO/EG-W(60:40) v/v% nanofluid deviates from the Nusselt number calculated from Gnielinski correlation. Nusselt number increases as thermophysical properties of nanofluid get improved.

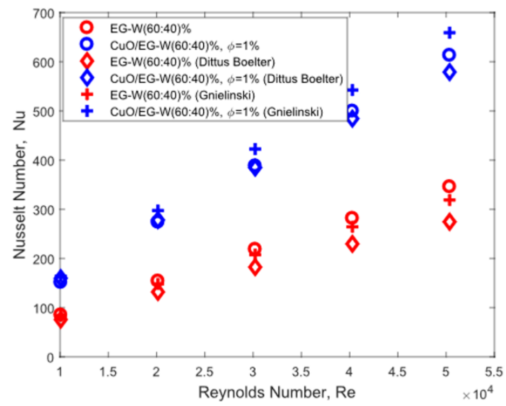

Fig. 4: Nusselt Number Vs. Reynolds Number

Fig.5 demonstrates that the pressure drop increases with the increase in Reynolds number. The pressure drop of nanofluid is maximum 0.24% higher than the base fluid for the same Reynolds number. Because of high viscosity, pressure drop increases in case of nanofluid for the same Reynold number as base fluid. Fig. 6 illustrates that pumping power per unit length for nanofluid decreases than base fluid for the same Reynolds number. As a result, volumetric flow decreases for the same Reynolds number.

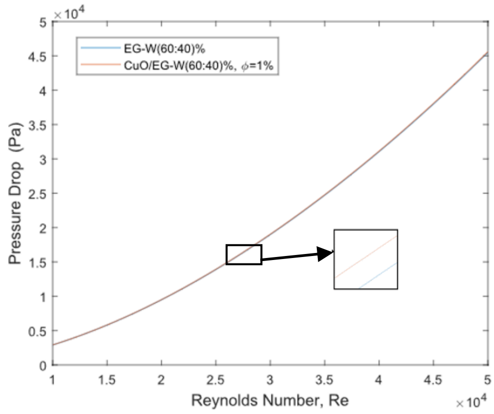

Fig. 5: Pressure Drop Vs. Reynolds Number

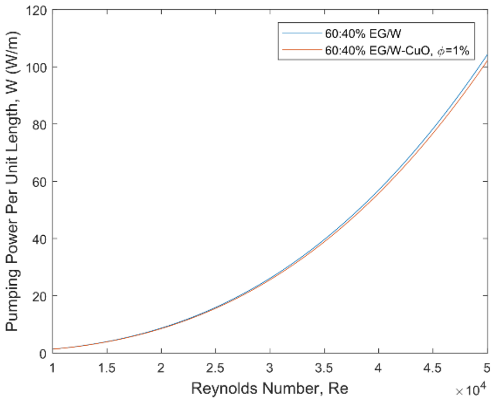

Fig. 6: Pumping Per Unit Length Vs. Reynolds Number

Fig. 7 and Fig. 8 demonstrate the effect of heat transfer coefficient and Nusselt number with pumping power per unit length. These figures also illustrate that higher pumping power per unit length is required for higher heat transfer coefficient and Nusselt number. Pumping power per unit length for 1% volume fraction CuO/EG-W (60:40) v/v% nanofluid is comparatively less EG-W (60:40) v/v% to get the same heat transfer coefficient and Nusselt number. Hence, nanofluid can increase the effectiveness of the cooling system which can save much power.

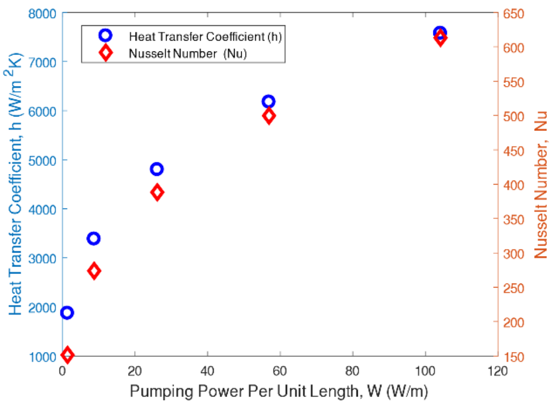

Fig. 7: Heat Transfer Coefficient and Nusselt Number Vs Pumping Power Per Unit Length of CuO/EG-W (60:40) v/v%

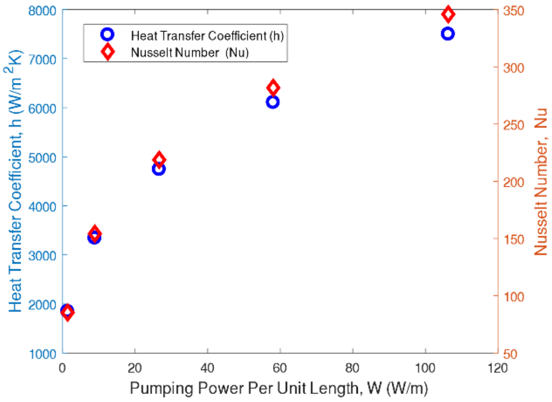

Fig. 8: Heat Transfer Coefficient and Nusselt Number Vs Pumping Power Per Unit Length of CuO/EG-W(60:40) v/v%

5. CONCLUSION

The present study investigated the pumping power of 1% volume fraction of CuO/EG-W (60:40) v/v% nanofluid. Heat transfer coefficient of CuO/EG-W (60:40) v/v% nanofluid is higher than EG-W (60:40) v/v%. Pumping power per unit length decreases for CuO/EG-W (60:40) v/v% nanofluid for the same Reynolds number of EG-W (60:40) v/v%. For the same heat transfer coefficient and Nusselt number, pumping power per unit length and volumetric flow rate of 1% volume fraction CuO/EG-W (60:40) v/v% nanofluid is less than EG-W (60:40) v/v%. Hence, much heat can be dissipated by less power consumption and also the compact cooling system can be designed.

7. REFERENCES

[1] S. M. Peyghambarzadeh, S. H. Hashemabadi, M. S. Jamnani, and S. H. Hoseini, “Improving the cooling performance of automobile radiator with Al2O3/water nanofluid”, *Journal of Applied Thermal Engineering*, vol. 31, no. 10, pp. 1833-1838, 2011.

[2] C. T. Nguyen, G. Roy, C. Gauthier, and N. Galanis, “Heat transfer enhancement using Al2O3-water nanofluid for an electronic liquid cooling system”, *Applied Thermal Engineering*, vol. 27, no. 8-9, pp. 1501-1506, 2007.

[3] S. Choi, “Nanofluids for improved efficiency in cooling systems”, *Heavy Vehicle Systems Review, Argonne National Laboratory, Argonne, IL*, 2006.

[4] Y. Xuan and Q. Li, “Heat transfer enhancement of nanofluids”, *International Journal of Heat and Fluid Flow*, vol. 21, no. 1, pp. 58-64, 2000.

[5] A.M. Hussein, K.V. Sharma, R.A. Bakar, K. Kadirgama, “The effect of nanofluid volume concentration on heat transfer and friction factor inside a horizontal tube”, *Journal of Nanomaterials*, vol. 27, no. 1, pp. 1-12, 2013.

[6] K. S. Hwang, S. P. Jang and S. U.S. Choi, “Flow and convective heat transfer characteristics of

water-based Al2O3nanofluid in fully developed laminar flow regime”, *International Journal of Heat and Mass Transfer*, vol. 52, no. 1-2, pp. 193-199, 2009.

[7] P.A. Ingole, S.M. Shinde, P.A. Patil, “Experimental Investigation of Pumping Power and Effectiveness of Car Radiator Using Al2O3”, *International Conference on Ideas, Impact and Innovation in Mechanical Engineering (ICIIIME 2017)*, ISSN: 2321-8169, vol. 5, Issue: 6, 135 – 141, 2017

[8] L. S. Sundar, M. H. Farooky and S. N. Sarada, “Experimental thermal conductivity of ethylene-glycol and water mixture based low volume concentration of Al2O3 and CuO nanofluids”, *International Communications in Heat Mass Transfer*, vol. 41, no. 1-2, pp. 41-46, 2013.

[9] Y. Xuan and W. Roetzel, “Conceptions for heat transfer correlation of nanofluids”, *International Journal of Heat and Mass Transfer*, vol. 43, no. 19, pp. 3701–3708, 2000.

[10] R. L. Hamilton and O. K. Crosser, “Thermal conductivity of heterogeneous two-component systems”, *IEC Fundamental*, vol. 1, no. 3, pp. 187–191, 1962.

[11] H.C. Brinkman, “The viscosity of concentrated suspensions and solution”, *Journal of Chemical Physics*, vol. 20, no. 4, pp. 571–581, 1952.

[12] C. F. Colebrook, “Turbulent Flow in Pipes, with Particular Reference to the Transition between the Smooth and Rough Pipe Laws”, *Journal of the Institute of Civil Engineers*, vol. 12, no. 8, pp. 393–422, 1939.

[13] B.S. Petukhov, “Heat Transfer and Friction in Turbulent Pipe Flow with Variable Physical Properties”, *Advances in heat transfer,* vol. 6, pp. 503–564, 1970.

[14] ASHRAE, Handbook Fundamentals, American Society of Heating, Refrigerating and Air-conditioning Engineers Inc., Atlanta, 2013

[15] D.R. Lide, CRC Handbook of Chemistry and Physics, eighty-fifth ed., CRC Press, Boca Raton, FL, 2005.

[16] Y. Li, J. Zhou, S. Tung, E. Schneider, S. Xi, “A review on development of nanofluid preparation and characterization”, *Powder Technology*, vol. 196, no. 2, pp. 89–101, 2009.

[17] V. Gneilski, “New equations for heat and mass transfer in turbulent pipe flow and channel flow”, *Int Chem Eng*, vol. 16, no. 2, pp. 359–368, 1976.

8. NOMENCLATURE

Symbol	Meaning	Unit
A	Area	(m^2)
V	Velocity of fluid	(m/s)
f	Friction factor	Dimensionless
Re	Reynolds number	Dimensionless
h	Heat transfer coefficient	$W/m^2.K$
Nu	Nusselt number	Dimensionless
Φ	Volume concentration	
ρ_{nf}	Density of nanofluid	kg/m^3
μ_{nf}	Dynamic viscosity of nanofluid	$N.s/m^2$
Cp_{nf}	Specific heat capacity of nanofluid	KJ/Kg.K
K_{nf}	Thermal conductivity of nanofluid	W/m.K
ΔP	Pressure drop	N/m^2
D_h	Hydraulic diameter	m
L	Length	m
W	Pumping power per unit length	W
Q_{nf}	Heat transfer	W
T_{bi}	Bulk temperature of inlet fluid	K
T_{bo}	Bulk temperature of outlet fluid	K
m_{nf}	mass flow rate of nanofluid	Kg/m^3